An Investigation into the Thermal Comfort of a conceptual Helmet Model Using Finite Element Analysis and 3D Computational Fluid Dynamics

Cerys E. M. Bandmann, Mohammad Akrami*, Akbar A. Javadi

Department of Engineering, College of Engineering, Mathematics, and Physical Sciences

University of Exeter, Exeter, United Kingdom

*Corresponding Author

Dr Mohammad Akrami, m.akrami@exeter.ac.uk

Keywords: Helmet ventilation, finite element analysis

Word count (introduction through conclusion): 3321

Submitted as an *Original Article*

Submitted to the *Journal of Industrial Ergonomics*

Abstract

A common reason for the reluctance to wear protective headgear during different sports activities like skating or biking is the thermal discomfort to the user caused by heat accumulation within the helmet. A review of existing literature revealed the potential to improve thermal comfort of helmets through convective heat transfer, most often achieved through passive ventilation. This paper aims to investigate areas of high heat concentration in the helmet and examine the effect of various hole configurations on the ventilation performance within the helmet. The thermal comfort properties of skate-style helmets are investigated using computational analysis in the form of finite element analysis and 3D computational fluid dynamics.

In order to identify areas of naturally high heat concentrations inside the helmet, a baseline conceptual helmet was generated in SolidWorks and a finite element analysis was undertaken in the form of a steady-state thermal study in ANSYS Workbench. Next, a 3D computational fluid dynamics investigation was performed on a range of concept designs developed from the baseline model, representing different hole configurations for three general hole locations – front, back and side. The best performing concept designs were then combined into a single model and tested. Flow speeds were measured at set probe points for four individual cross-sections for all the test concept designs. Using the collected data, the ventilation performance of the various concept designs was discussed relative to the baseline model and justified.

The computational studies revealed trends between the general hole locations and the local ventilation efficiency, as well as differences between the individual concepts tested for each location. Key findings include holes at the rear being the most beneficial to overall helmet ventilation when compared to front and side holes. Furthermore, all hole locations were found to predominantly affect the flow speeds in the central and upper frontal regions of the helmet, with little impact on the parietal and occipital lobe regions. The best hole configurations were found to be three holes, one hole and two holes for the front, back and side locations respectively. It was shown that combining the strongest individual concept designs does not necessarily lead to a superior helmet design in terms of ventilation performance.

1. Introduction

A review of existing helmet designs and research revealed the inherent issue of thermal discomfort during usage and highlighted the scope for an investigation into their ventilation characteristics. As heat is dissipated from the head of the user, it accumulates inside the helmet, raising the temperature and increasing the thermal discomfort experienced by the wearer. This discomfort is likely to negatively impact the readiness to wear the protective headgear, which could lead to severe head injuries or even fatal consequences in the event of a fall. In order to counteract this unwanted rise in temperature, ventilation is a commonly used tool to prevent stagnant air and encourage airflow through the helmet, introducing cooling air into the system, and thereby removing the warmer air. This study attempts to investigate the effects on the ventilation properties of the helmets of various hole arrangements placed at three different key locations, with the aid of computer aided design and computational simulation software.

Various researchers have studied the effect of ventilation holes on the convective heat transfer of the head, as well as their efficiency in ventilating the helmet interior. Ventilation is important to the thermal comfort of the user as it enables the heat loss through forced convection, promotes the evaporation of sweat, and removes this from the proximity to the head, which would otherwise increase the humidity inside the helmet [1]. The psychophysical tests showed that ventilation contributes in greater helmet comfort [2]. It is suggested that there is a significant optimisation potential within the basic structure represented in modern bicycle helmets [3]. A comparative study from 2015 on thermal properties of cricket helmets showed significant benefits to the head temperature of forced convection, with a decrease of 5°C [4]. In recent years, protective helmets have been developed with an increased number and size of ventilation holes in the shell [1], intending to give the user the perception of good ventilation [5]. However, the efficiency of the chosen hole sizes and positions is often disregarded, posing a threat to the user, as it has been established that increasing the number of holes results in less damping in a crash, while not necessarily improving ventilation. Therefore, there is a need for detailed evaluation of the usefulness of individual vents; a careful selection of vent size, number and location could simultaneously improve thermal as well as the mechanical requirements [6].

Previous research has hypothesized that the main determinant for coolness in the venting of helmets is the total area of front vents [5, 7, 8]. This could be confirmed by a study [3], attempting to relate the ventilation efficiency to the size and number of ventilation holes.

However, the projected inlet ventilation hole areas could only be shown to affect the ventilation of the frontal areas of the head and did not relate to the rear ventilation efficiency, which remained poorly ventilated [4, 5, 9]. While the presence of ventilation holes at the rear did not explicitly impact the local ventilation efficiency in that area, they are nonetheless recognized as significant components of the design, being integral to the successful ventilation of the helmet [3]. Per an investigation of firefighter helmets by Reischl in 1986 [10], side ventilation holes resulted in a cooler helmet than the unventilated version. However, it has been acknowledged that certain vent configurations imposed a negative effect on forced convection, such as holes in the middle of a helmet versus top of a helmet, which interrupted the function of the air channels [3, 5], as well as holes at the top, encouraging premature exiting of the airflow, prior to full exploitation of its cooling properties [3].

An observation made during the literature review stage revealed the abundance of comparative, experimental studies between existing models when attempting to assess ventilation properties. However, a fundamental flaw in this methodology is the influences of multiple other factors on the airflow, such as general size, shape, inner lining, fitting system, air gap, combinations of holes etc. This study aims to target these sources of error by producing a standard parametric helmet model, with the only independent variable being the hole configuration throughout all tests, and using controlled numerical methods to evaluate the differences between hole configurations in isolation.

2. Methodology and Theory

2.1. CAD Model of Baseline Helmet

In order to run simulations, a parametric helmet model was generated in SolidWorks [11] using true head dimensions [12] and skull profile images [13] for a more accurate analysis and better adjustability (Figures 1-6).

2.2. Heat Study

In order to evaluate the heat distribution and identify areas of naturally high heat concentration (HHC) resulting from radiating heat from the human head, a steady-state thermal study was carried out and the results are illustrated in figure 7. The maximum temperature rise in this study is comparable to the literature [22] in order to validate the results. The simulation setup was such that a temperature was applied to the inner surface of the helmet, simulating the effect of the head being in contact with the inner surface. The outer surface dissipated heat to the environment (22°C) via convection. It is assumed that the inner surface of the helmet is exposed to the average skin temperature of the head (37°C [14]). To establish the heat transfer coefficient for the heat being dissipated from the helmet to the environment, Equation 1 was used.

$$h_c = 10.45 - v + 10.v^{\frac{1}{2}} \qquad \text{Equation 1}$$

Where h_c is the heat transfer coefficient, and v is the relative speed of the object through the air (m/s) [15]. Assuming a relative airspeed of 1 m/s (still conditions), h_c has been found to be 19.45 W/m^2K^{-1}. The standard tetrahedral elements were used with an adaptive sizing function and minimum edge length of 1.085mm. A mesh convergence study was undertaken, and, based on this, an element count of 5,949 was applied. The effects of solar radiation have been omitted for the purpose of this study. The material was set as carbon fibre, with a material conductivity of 21 W/mK. The results obtained from this study are best represented in visual form (Figure 7), revealing areas of naturally HHC.

2.3. Airflow Study

A simulation was undertaken in which air flow was simulated through the helmet assembly and the airspeed was measured between the helmet and head. In this study, the focus was on frontal flow (0° tilt angle), as this is the most common airflow experienced by skaters. The airspeed was assumed to be 5m/s, based on an estimation of airspeed around cyclists when travelling at "average speed" in a city, as this is closely related to the speed of skaters [16].

In order to systematically structure the investigation, three different hole configurations were designed (with one, two and three holes) for each of the three general locations (front, back and side), as well as a final concept (C1), which combines the best performing designs (Table 2). Holes were kept relatively small, so not to compromise structural integrity [6], and were extruded in the direction of airflow to maximize the projected hole area [17]. The essence of ventilation from the side vents have also been advised based on the British/European standards BS/EN 397 [21].

An airflow cylinder was constructed, to act as the framework for the flow simulation (Figures 8-9). The front face was set as the velocity inlet, and the rear end as the pressure outlet; air flow was then simulated through the cylinder. A tetrahedral CFD mesh of approximately 460,000 elements was applied, and the proximity function was used to focus the mesh around the area of interest. The simulation model assumes no hair and an inner lining of the same shape as the outer shell as the effects of large amounts of hair was discussed in another experimental study [19] which reduced down the cooling power. Furthermore, the helmet is considered to have a suspension system to permit airflow between it and the head; this is to simplify the model, so as to allow the outer shell geometry to be tested in isolation, as this is the primary focus of the study.

In order to gather airflow speed data, four standard representative cross-sections were selected (assuming symmetry w.r.t. the central plane). Fixed probe points were plotted on each of the four cross-sections following the curved path of interest (Figures 10-13), and flow speed data was collected from these points after each simulation (Figures 14-29). These are designed based on the experimental data collections on the poorly ventilated locations from the literature [20].

To facilitate interpretation of results, concept 0 (unventilated) was set as the baseline model, and all collected data for the ventilated concept designs were scaled accordingly. Furthermore, the airspeeds for the individual probe points were weighted according to the heat study results in order to indicate areas of elevated ventilation importance. Averages (relative to the baseline model) of the concept designs for each probe point, each cross-section, as well as the overall helmet, were calculated, endeavouring to estimate and compare the ventilation successes of the individual designs.

3. Results and discussion

3.1 Heat Study

A clear pattern can be identified on the outer surface of the helmet, indicating local ability to dissipate the heat being exerted to the inner surface (see Figure 7). Although the absolute differences in temperature rise are minimal, it indicates areas naturally prone to heat concentration. A possible reason for the relevant areas showing lower temperature gradients could be the curvature of the surface. The greater the curvature, the bigger the ratio of the surface of the heat source to heat dissipation surface, resulting in less heat accumulation, and a relatively cooler area of the helmet. The probe points on the individual cross-sections corresponding to the heat concentration regions are identified (Table 1).

3.2 Airflow Study

3.2.1 Location Comparison

On average, front holes appear not to have a beneficial effect on the flow in the helmet, apart from one configuration (F3). Front holes appear to have worsened flow in the majority of CS0 and CS+2 (-10.9% and -4.6% respectively). In contrast, front holes generally appear to have a positive effect on the flow speeds for CS+1 and CS+3, with overall average improvements of +13.0% and +3.6% over the baseline concept respectively. Specifically, areas of increased ventilation performance appear to be the lower central and upper left and right frontal regions of the head, while the worse performance was observed consistently in the parietal/occipital lobe region of the head. A possible reason for this observation may be due to the loss of energy experienced by the air during ventilation [5], which is potentially amplified by elevated entry speeds resulting from front holes.

The back hole configurations seemed to be beneficial overall, showing improvements relative to the baseline model in all four cross-sections. Nonetheless, patterns of adverse effects on flow in the parietal and occipital regions of the head were still observed, as well as its effect on CS+2. Overall, areas of increased ventilation performance are found in the central and upper sides of the frontal region, as well as in the region where the parietal and temporal lobes meet, while flow speeds tend to decrease towards the lower occipital lobe regions for most cross-sections. Furthermore, the margins of improvement observed in two of the three back hole concepts are rather significant, indicating the back of the helmet is the most influential of the three locations for ventilation holes.

In general, side holes seem to marginally benefit general helmet ventilation, supporting existing study findings by Reischl [18], with only one of the three concepts showing a worse average than the baseline model. However, side holes show the lowest marginal changes relative to other hole locations, indicating limited influence. Overall, areas of increased flow speeds shift towards the rear as the cross-section increases the distance to the central plane. While CS0 shows high flow speeds in the lower frontal area, CS+1 and CS+2 show improvements in the upper frontal region and top region respectively. As observed for other hole location, adverse effects are seen to be caused by the rear parietal and occipital lobe regions of the head for all cross-sections. (Table 3, Figures 30-33)

3.2.2 Probe Point Sensitivity

As a method of quantifying and evaluating the effect of different general hole locations (front, back side), as well as identifying areas of high variation, the variance of the flow rate at each of the probe points was calculated and plotted for all three hole locations. Figures 34-37 reveal all hole locations predominantly affecting the flow in the frontal regions of the head (as observed by De Bruyne et al. [5]) on the central cross-section, but the area of high variation appears to extend to central (top of head) regions as the distance to the central cross-section increases. It is particularly noticeable that in general the back and side holes tend to result in larger variance in the frontal regions, while frontal holes appear to predominantly affect probe points in the centre of the flow path. Relatively little effect could be identified in varying hole configuration in different locations on flow speeds towards the rear of the helmet. Upon more detailed inspection, the variance towards the rear of the helmet was consistently of negative nature, which is likely due to the phenomenon described by Brühwiler et al. [3], whereby the airflow takes the "easiest" way through the system and thereby exits the helmet at the earliest opportunity. While C0 did not permit any early exiting due to the lack of ventilation holes, the concept models may have encouraged this effect. Alternatively, the energy loss of the airflow may be amplified by new inlets causing higher speeds of entry and greater interference [5].

3.2.3 Concept Comparison

Comparing the front hole configurations, F3 demonstrates the most favourable overall average (+5.5%). This dominance of F3 supports existing theories on the positive relationship between projected inlet area and ventilation efficiency [3, 5, 7, 8].

When assessing the back hole configurations, B1 is determined to be the best design, based on the overall average improvement of +7.3%. B2 demonstrated the weakest performance; the reason for this poor performance is unclear, however, it can be speculated that there may be a relationship between ventilation efficiency of rear holes and their proximity to one another.

S2 has the best performance consistently of the three side hole configurations, with an improvement of 2.8%. S1 shows the weakest performance; the reason for this poor performance is unclear, however, it can be speculated that there may be a relationship between ventilation efficiency of rear holes and their proximity to one another.

3.2.4 Combination of Strongest Concepts

Although the combination concept design had an overall helmet average greater than that of the unventilated design (+4.7%), it was still lower than that of certain concept designs, such as F3, B1 and B3. The cross-section averages for this concept design showed improvements for certain cross-sections (CS+1 and CS+3), but little change and even adverse effects for other cross-sections (CS0 and CS+2 respectively). This observation demonstrates and confirms the phenomenon outlined in various papers, whereby more holes do not automatically improve ventilation [6], and that holes at different locations cause complex interactions, having influences on airflow and flow paths. It is apparent that the reason for the improved ventilation performance of certain isolated hole configurations is nullified through the addition of other holes. Holes at varying distances from the front may act as additional inlets, either adding to the flow speed or countering it or as additional outlets, allowing early exiting of the cooling air prior to full exploitation [17]. Certain arrangements of secondary holes can exacerbate the cooling power of the helmet [3]. Overall, further studies with controlled variation of hole combinations would be required in order to determine ideal hole combinations for comprehensive ventilation improvement.

4. Conclusion and suggestions for Future Research

In general, holes at the rear of the helmet proved to show the best average flow speeds for the tested concept designs compared to hole configurations at other key locations, as well as the largest variation at probe points, implying more efficient ventilation and high probe point sensitivity of the hole location.

All hole locations predominantly affect flow speeds in the frontal regions of the helmet on the central cross-section, but the area of high variation appears to tend towards the central regions of the flow path as the distance to the central cross-section increases.

While the back and side holes mainly influence the centrally located cross-sections, the effect of side holes on flow speeds increases with distance from the central plane. Back and side holes tend to have the largest effect on flow speeds in the frontal areas, while frontal holes affect regions towards the centre of the flow path (intersection between frontal and parietal lobes). Based on the simulation results, F3, B1 and S2 were identified to be the best concepts for the front, back and side locations respectively, but were shown to have individual strengths and weaknesses, particularly in targeting regions identified as naturally higher heat concentrations. Also, it is showed that the combining the most successful concept designs does not necessarily lead to a superior design with respect to ventilation properties. Based on the assumptions and limitations of the current study, future works should include:

- *Increase projected inlet area to increase flow rate:* As suggested by G. De Bruyne [5], increasing hole sizes would encourage more airflow and improve ventilation. However, the effect of hole size on impact safety should always be considered. Also, the relationship between hole size, shape and ventilation efficiency needs to be investigated in future studies. In this current study, only the rectangular shapes were assumed for analysis, as different helmets have different shape and sizes for the holes.
- *Adjust the orientation of inlet vents to increase the mass flow rate of air inside the helmet:* As suggested by Pinnoji et al. [17], making the inlet slots tangential to the head form could smoothen the flow, so no vortex zone would form.
- *Adjust the shape of inlets:* It was observed in this study that the low height of the inlet slot hindered effective flow, and it is likely that airflow inside the helmet would have been greater if tall thin slots or round holes had been used.
- *Vary distance between holes and explore the effect on airflow:* Based on the findings of this study, it was observed that a possible reason for certain results may have been the distance between the holes.
- *Test top holes:* Holes at the top of the helmet were not tested in this research, and are worth further investigation.
- *Consider other factors in the airflow model, such as hair, inner lining, internal air channels and helmet straps:* To maintain a reasonable scope for this study, various elements were not addressed. Therefore, the scope for the development of the model has been identified. While

certain components may hinder/alter flow patterns, air channels appear to be instrumental in tackling the rear areas of low flow speeds [5].

- *Validate simulations experimentally:* Although this was beyond the scope of this study, potential for validation through experimental testing (e.g. tracer gas) emulating the computational simulations has been identified. This is in response to the acknowledgement of the software limitations.
- *Assess applicability of selected probe points:* In order to reduce the uncertainty of results, the selected probe points and flow patterns should be analysed and tested for their representative value, in order to assure representative points are selected.
- *Test more side hole configurations, with the focus on the relationship between hole proximity to the rear and overall helmet ventilation efficiency:* A pattern was identified in the data collected from side hole simulations, and it was speculated that this was related to the presence of a hole closer to the rear of the helmet.

Moreover, the effects of this conceptual design on the subject's metabolic performance, biometrics and psychophysics were not addressed due to the existed limitations which should be evaluated in future models.

Funding

This research did not receive any specific grant from funding agencies in the public, commercial, or not-for-profit sectors.

References

[1] Bogerd, C.P., Aerts, J.-M., Annaheim, S., Bröde, P., de Bruyne, G., Flouris, A.D., Kuklane, K., Mayor, T.S. and Rossi, R.M (2015) 'A review on ergonomics of headgear: Thermal effects', *International Journal of Industrial Ergonomics*, 45, pp. 1 12. Doi: 05.12.2016.

[2] Davis, G.A. et al. "Effects Of Ventilated Safety Helmets In A Hot Environment". International Journal of Industrial Ergonomics 27.5 (2001): 321-329. Web.

[3] Brühwiler, P. A. Et al. "Heat Transfer Variations Of Bicycle Helmets". Journal of Sports Sciences 24.9 (2006): 999-1011. Web. 22 Feb. 2017.

[4] Pang, Toh Yen et al. "A Comparative Study Of Vent Designs For Effective Ventilation In Cricket Helmets". Procedia Engineering 112 (2015): 395-399. Web. 22 Feb. 2017.

[5] De Bruyne, Guido et al. "Quantification Of Local Ventilation Efficiency Under Bicycle Helmets". International Journal of Industrial Ergonomics 42.3 (2012): 278-286. Web. 12 Feb. 2017.

[6] Van Brecht, A. Et al. "Quantification Of Ventilation Characteristics Of A Helmet". Applied Ergonomics 39.3 (2008): 332-341. Web. 20 Mar. 2017.

[7] "Bicycle Helmet History". Bhsi.org. N.p., 2016. Web. 11 Nov. 2016.

[8] Ellis, A.J., 2003. Development of Fundamental Theory and Techniques for the Design and Optimisation of Bicycle Helmet Ventilation (PhD thesis). RMIT University, Melbourne.

[9] Pang, Toh Yen, Aleksandar Subic, and Monir Takla. "A Comparative Experimental Study Of The Thermal Properties Of Cricket Helmets". International Journal of Industrial Ergonomics 43.2 (2013): 161-169. Web. 17 Feb. 2017.

[10] "Tour De France The Facts | Tour De Yorkshire". Letour.yorkshire.com. N.p., 2017. Web. 17 Mar. 2017.

[11] Solidworks. Dassault Systèmes, 2017. Print.

[12] Poston, A. (2008) Human Engineering Design Data Digest. Washington, DC: DoD HFE TAG.

[13] "Skull". Rocío Ocaña. N.p., 2017. Web. 5 Jan. 2017.

[14] Edwards, M. and Burton, A.C. (1960) Temperature distribution over the human head, especially in the cold. Journal of Applied Physiology, pp 209-2011.

[15] Convective Heat Transfer (2017) Available at http://www.engineeringtoolbox.com/convective-heat-transfer-d_430.html (Accessed: 27 February 2017).

[16] "Hur Fort Cyklar Folk? | Trafik I Stan". Trafikistan.se. N.p., 2017. Web. 15 Apr. 2017.

[17] Pinnoji, P.K., Haider, Z., Mahajan, P., 2008. Design of ventilated helmets: computational fluid and impact dynamics studies. Int. J. Crashworthiness 13, 265-278.

[18] U. Reischl, 1986. *Fire Fighter Helmet Ventilation Analysis*. American Industrial Hygiene Association Journal, 47 (8) (1986), pp. 546–551

[19] Brühwiler PA, Buyan M, Huber R, Bogerd CP, Sznitman J, Graf SF, Rösgen T. Heat transfer variations of bicycle helmets. Journal of sports sciences. 2006 Sep 1;24(9):999-1011.

[20] Van Brecht A, Nuyttens D, Aerts JM, Quanten S, De Bruyne G, Berckmans D. Quantification of ventilation characteristics of a helmet. Applied Ergonomics. 2008 May 1;39(3):332-41.

[21] British Standards Institution [BSI] 1995, BS EN 397: 1995. Specification for Industrial Safety Helmets, (London: BSI).

[22] Hsu, Yeh-Liang, Chi-Yu Tai, and Ting-Chin Chen. "Improving thermal properties of industrial safety helmets." *International Journal of Industrial Ergonomics* 26.1 (2000): 109-117.

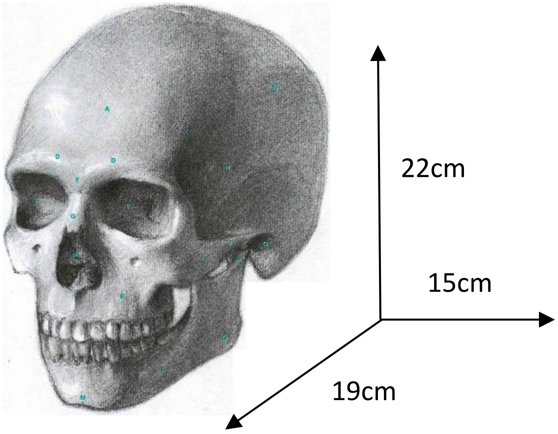

Figure 1: showing skull dimensions applied to profile images

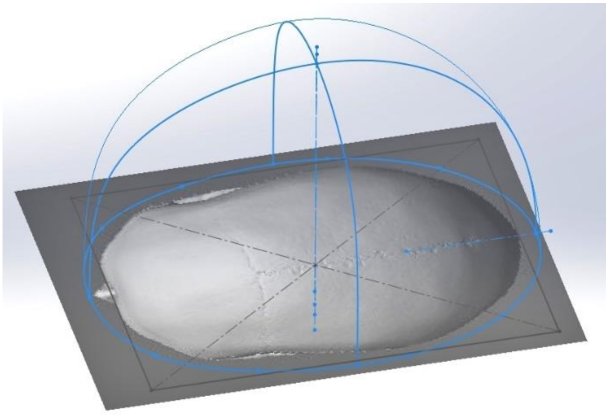

Figure 2: Combining helmet profiles

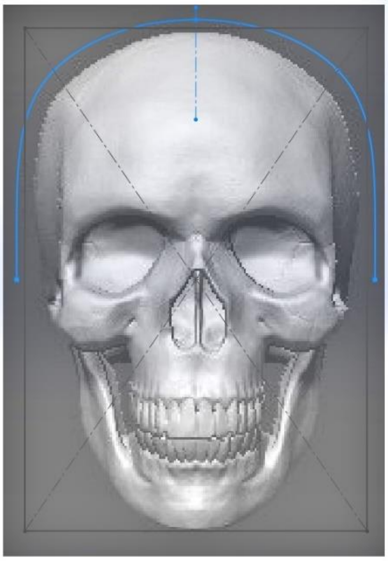

Figure 3: Front sketch for helmet generation

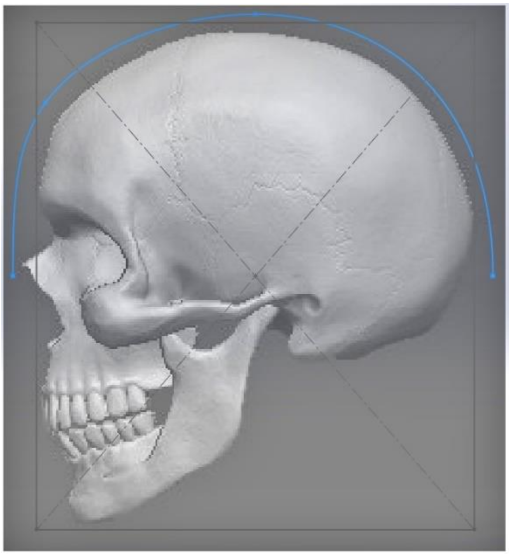

Figure 4: Side sketch for helmet generation

Figure 5: Top sketch for helmet generation

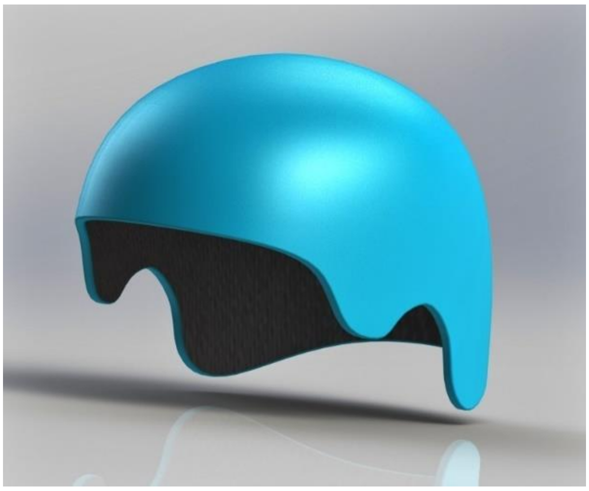

Figure 6: Baseline model "Concept 0"

Table 1: Regions of relatively low and high heat concentrations

Cross-section	Regions that have relatively lower heat concentration (Based on figures 10-13)	Regions that have relatively higher heat concentration (Based on figures 10-13)
CS0	1-6 & 30-33	7-29
CS+1	1-6 & 22-24	7-21
CS+2	1-5, 8-11 & 17-19	6-7 & 12-16
CS+3	1-2 & 9-13	3-8

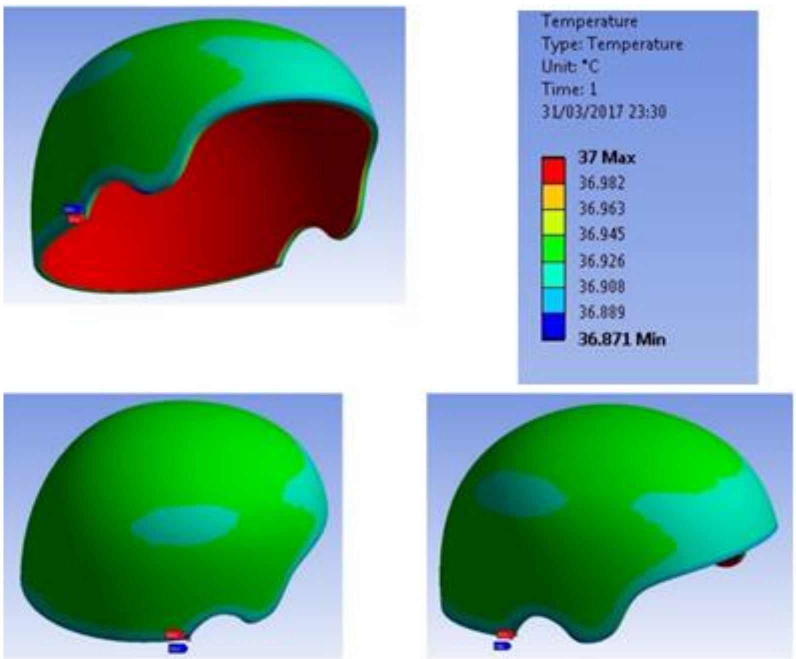

Figure 7: Heat distribution within the conceptual helmet model

Table 2: describing concept designs

Location	Concept Name	Hole configuration
Front	F1	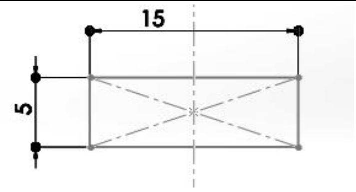
	F2	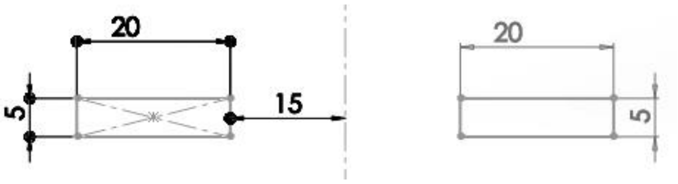
	F3	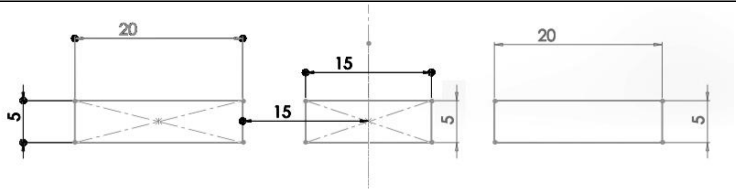
Back	B1	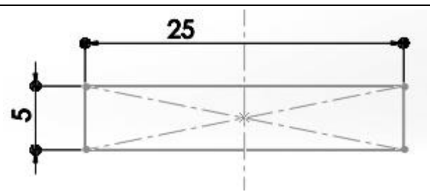
	B2	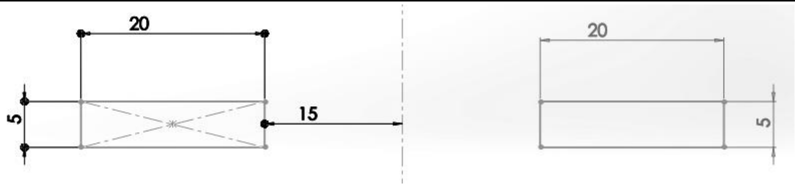
	B3	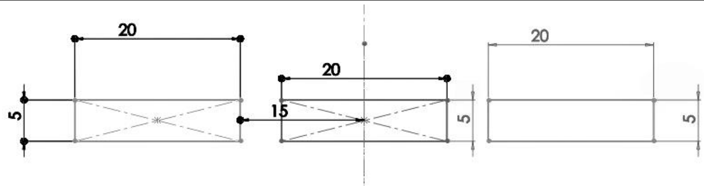
Side	S1	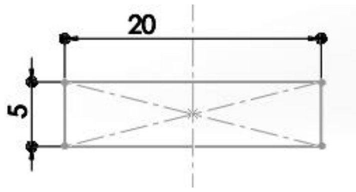
	S2	
	S3	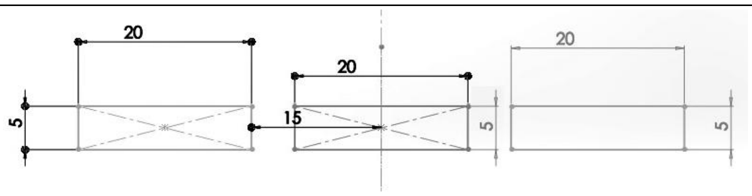
n/a	C1	Combination of F3, B1 and S2

Figure 8: An example of the helmet-head manikin assembly for concept C1

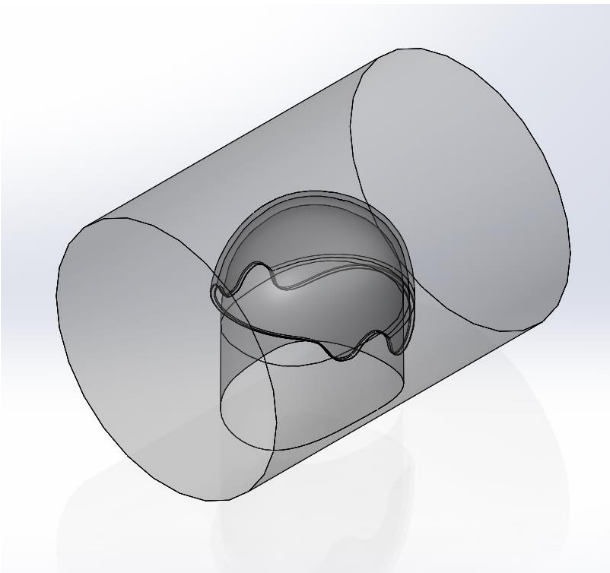

Figure 9: showing shaped airflow cylinder, with
cavities in place of the helmet and head manikin

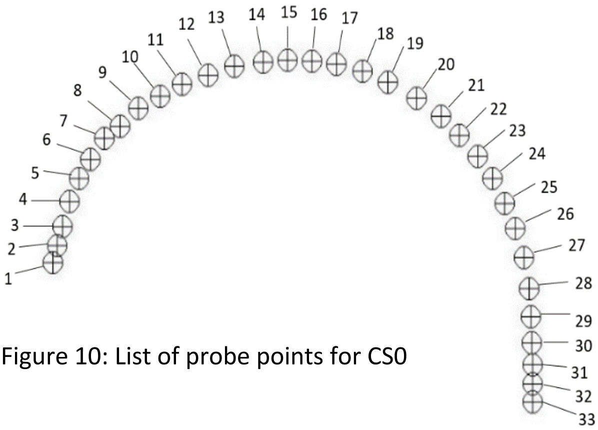

Figure 10: List of probe points for CS0

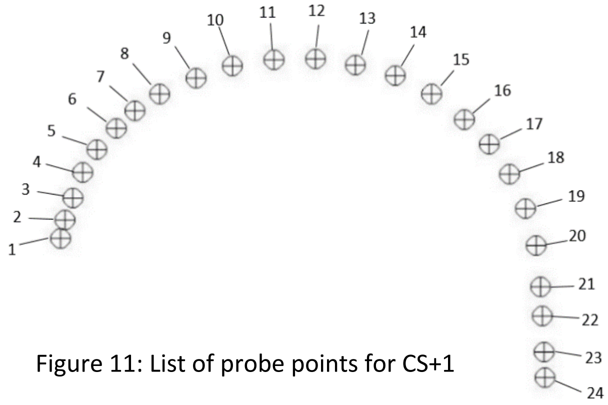

Figure 11: List of probe points for CS+1

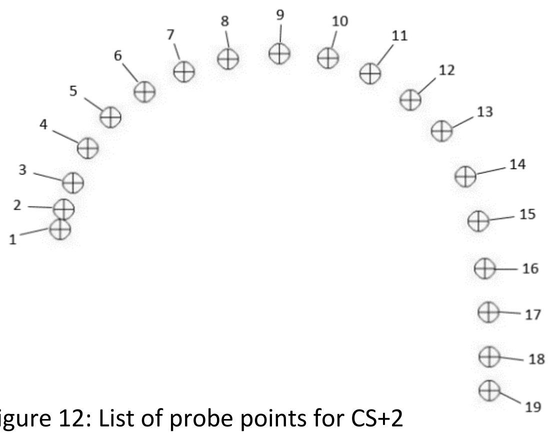

Figure 12: List of probe points for CS+2

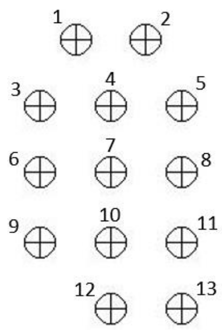

Figure 13: List of probe points for CS+3

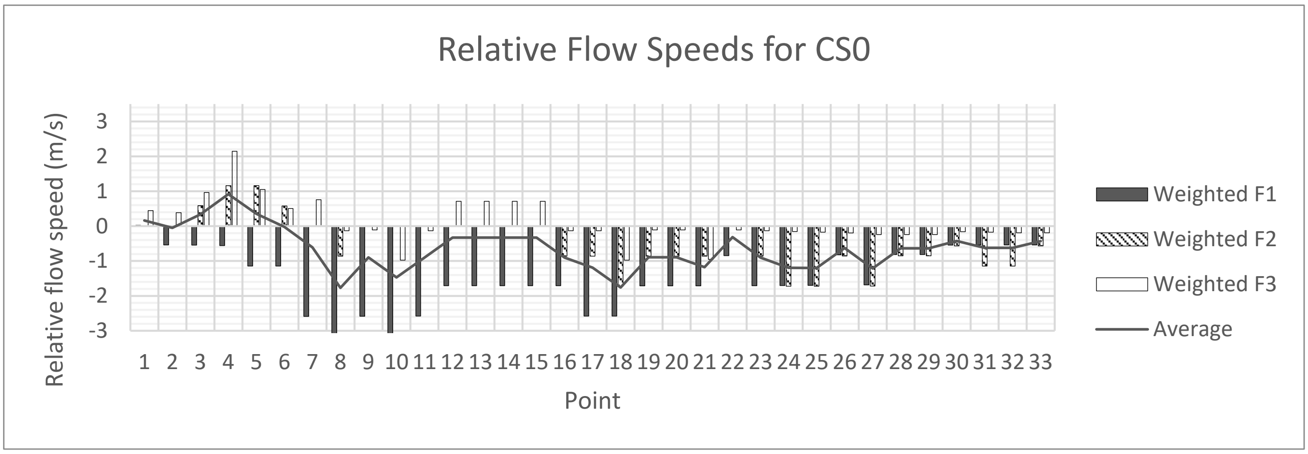

Figure 14: Weighted relative flow speeds for CS0 cross-section of FRONT hole

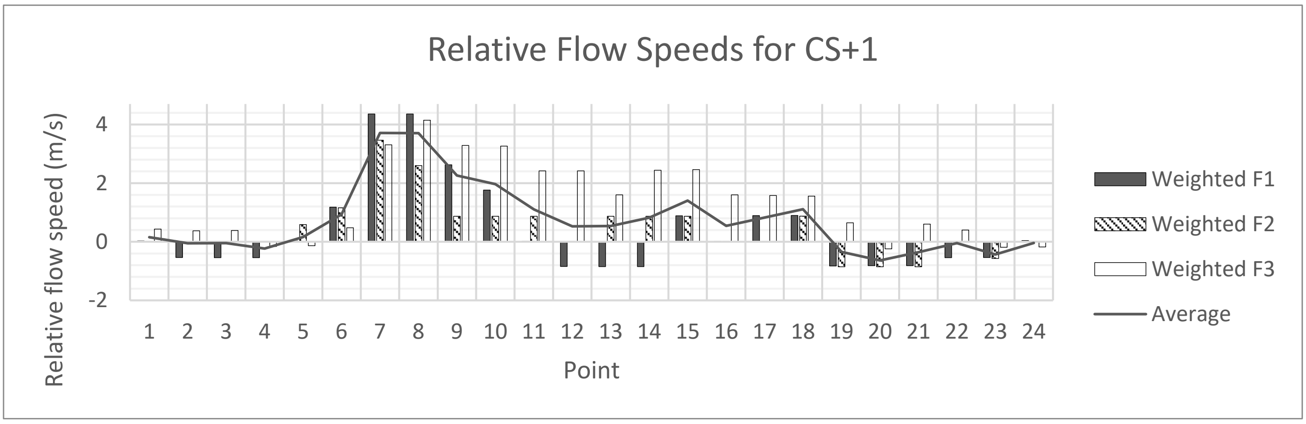

Figure 15: Weighted relative flow speeds for CS+1 cross-section of FRONT hole configurations

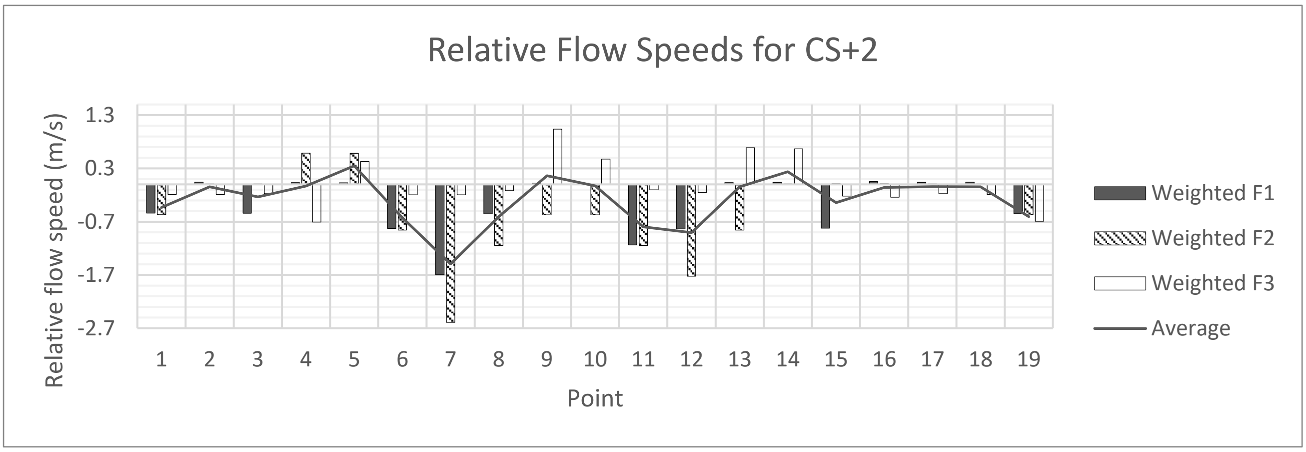

Figure 16: Weighted relative flow speeds for CS+2 cross-section of FRONT hole configurations

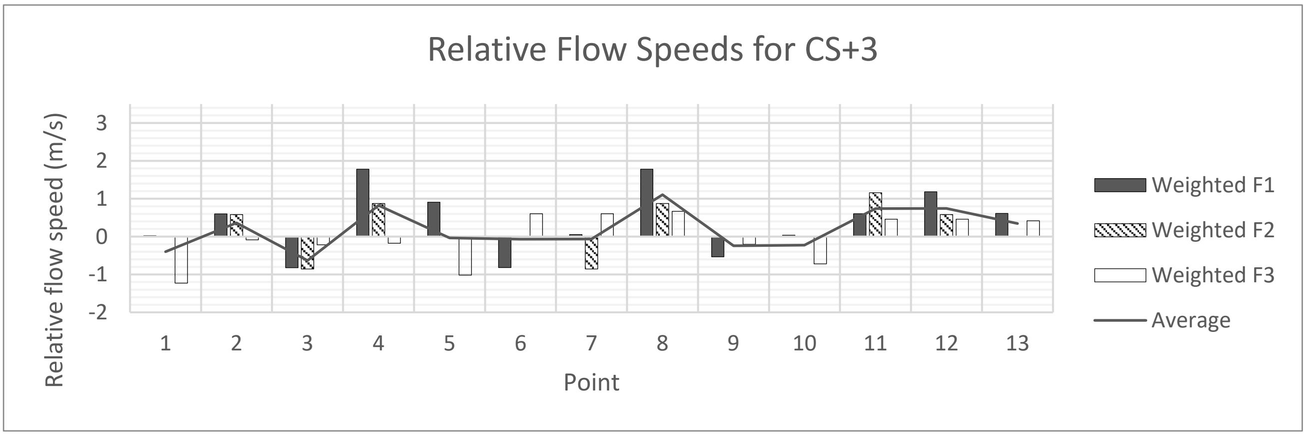

Figure 17: Weighted relative flow speeds for CS+3 cross-section of FRONT hole configurations

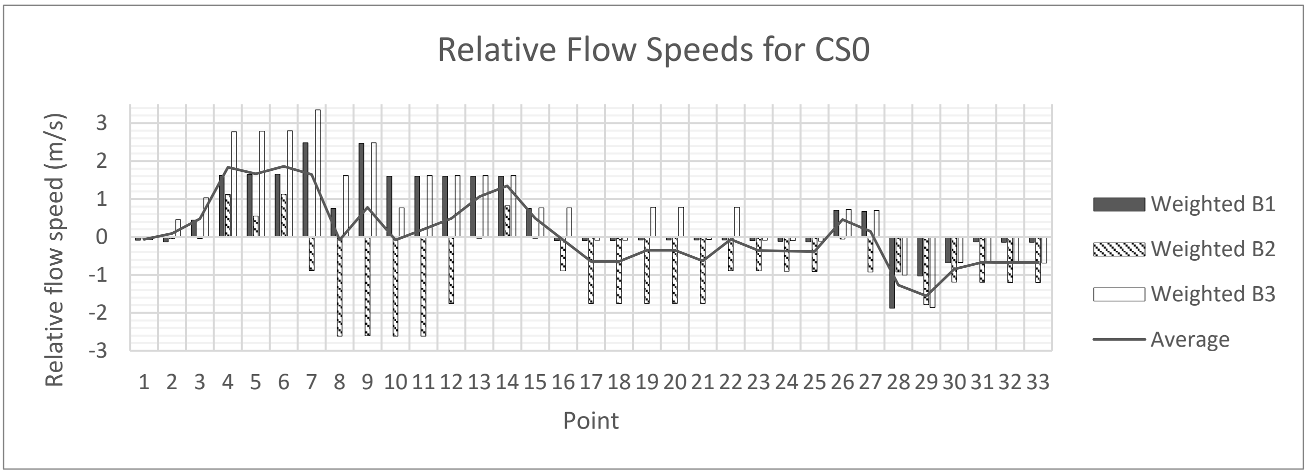

Figure 18: Weighted relative flow speeds for CS0 cross-section of BACK hole configurations

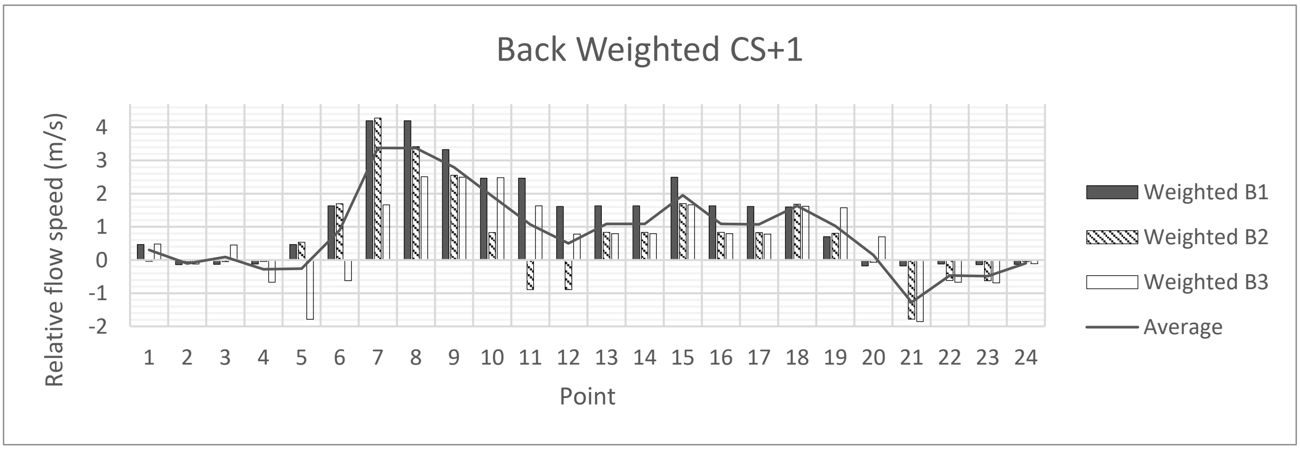

Figure 19: Weighted relative flow speeds for CS+1 cross-section of BACK hole configurations

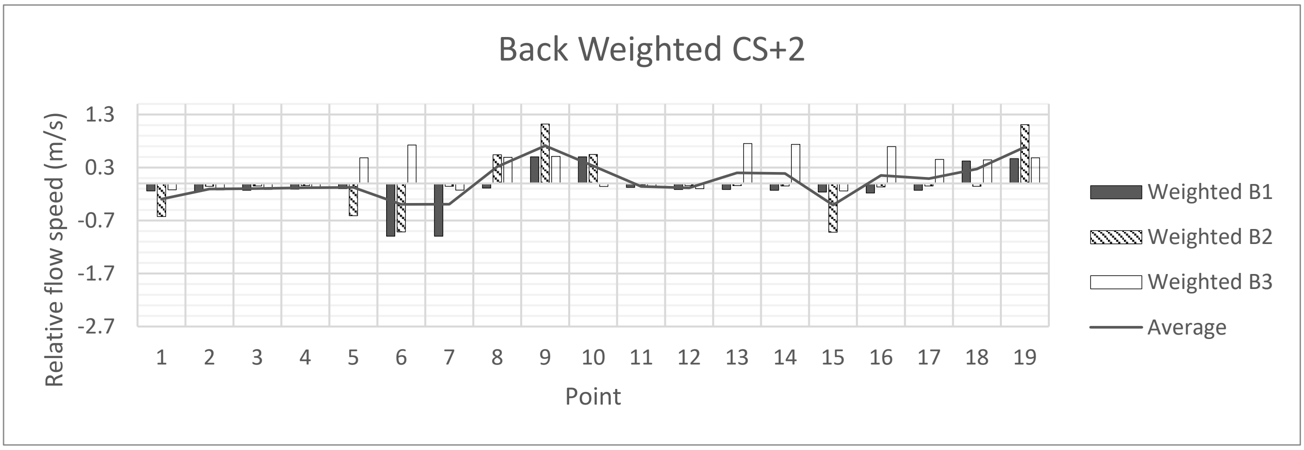

Figure 20: Weighted relative flow speeds for CS+2 cross-section of BACK hole configurations

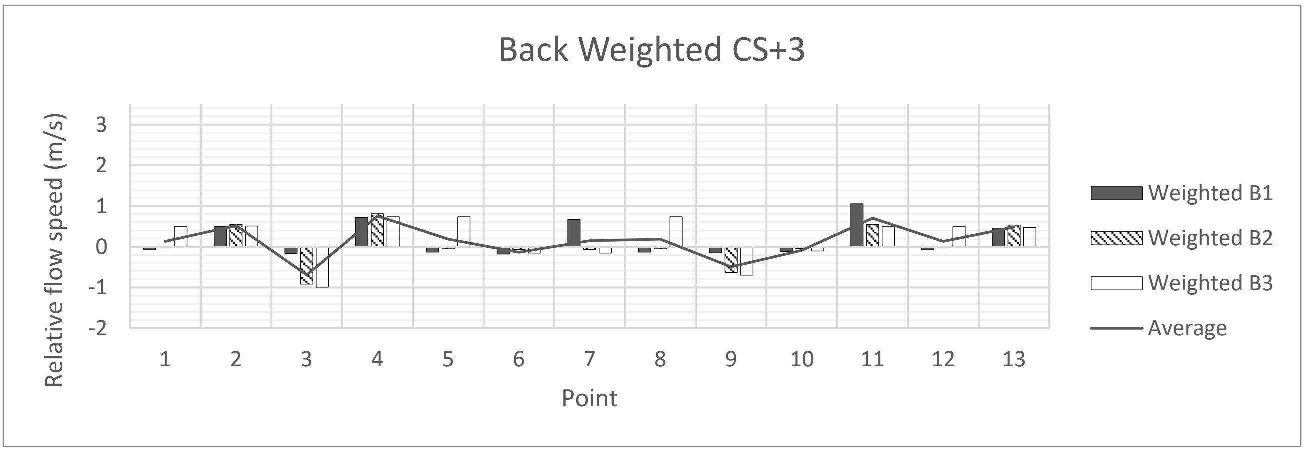

Figure 21: Weighted relative flow speeds for CS+3 cross-section of BACK hole configurations

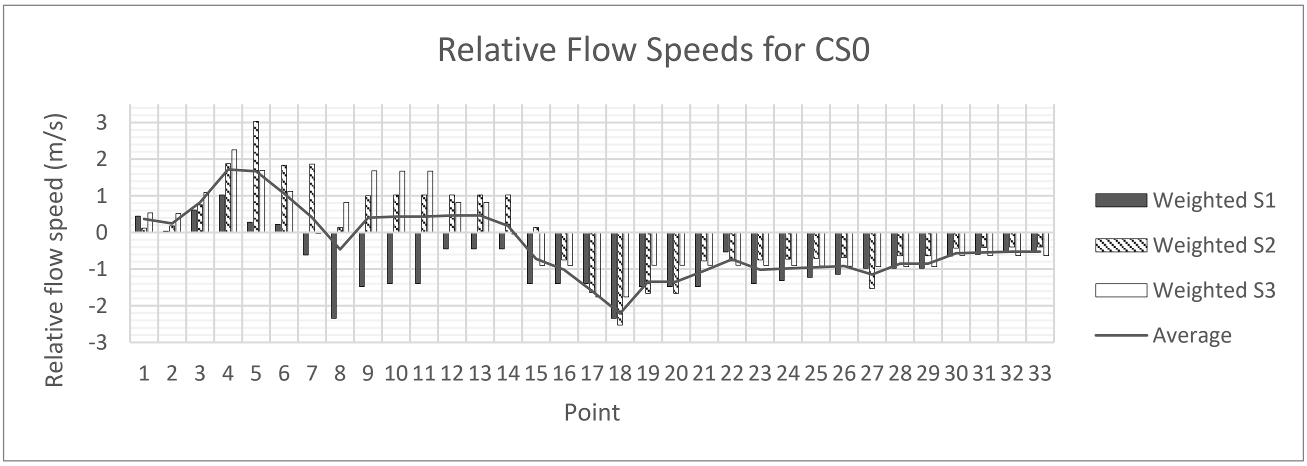

Figure 22: Weighted relative flow speeds for CS0 cross-section of SIDE hole configurations

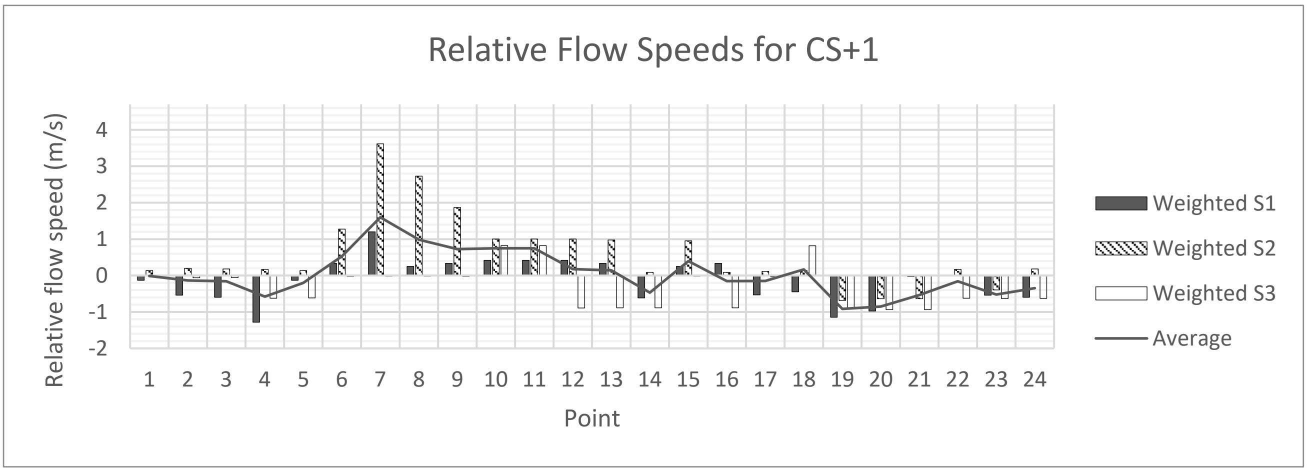

Figure 23: Weighted relative flow speeds for CS+1 cross-section of SIDE hole configurations

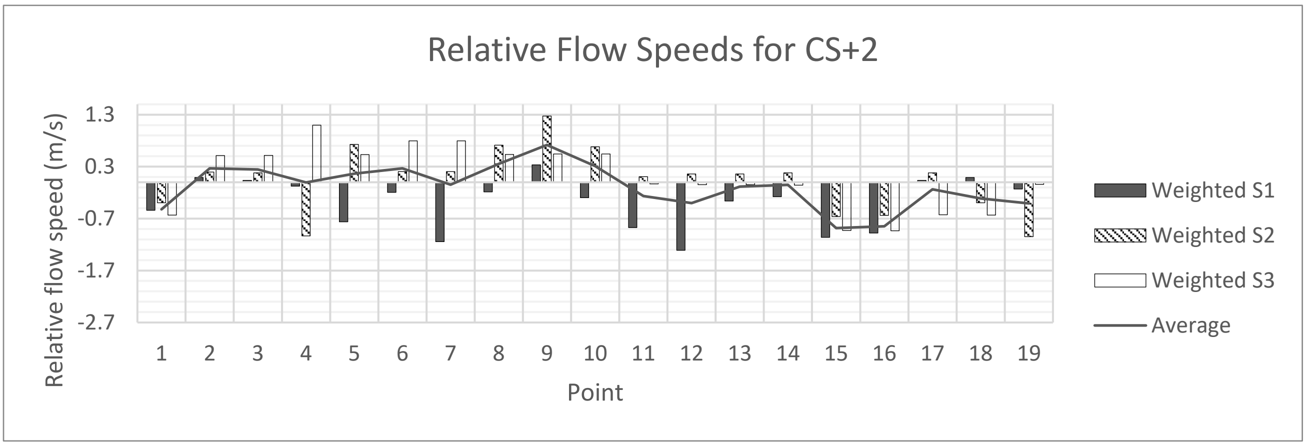

Figure 24: Weighted relative flow speeds for CS+2 cross-section of SIDE hole configurations

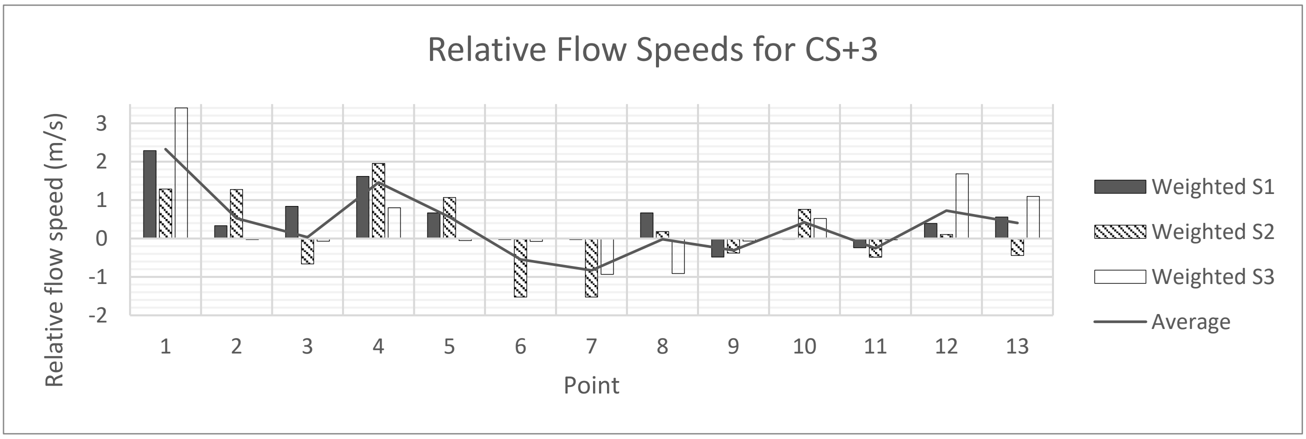

Figure 25: Weighted relative flow speeds for CS+3 cross-section of SIDE hole configurations

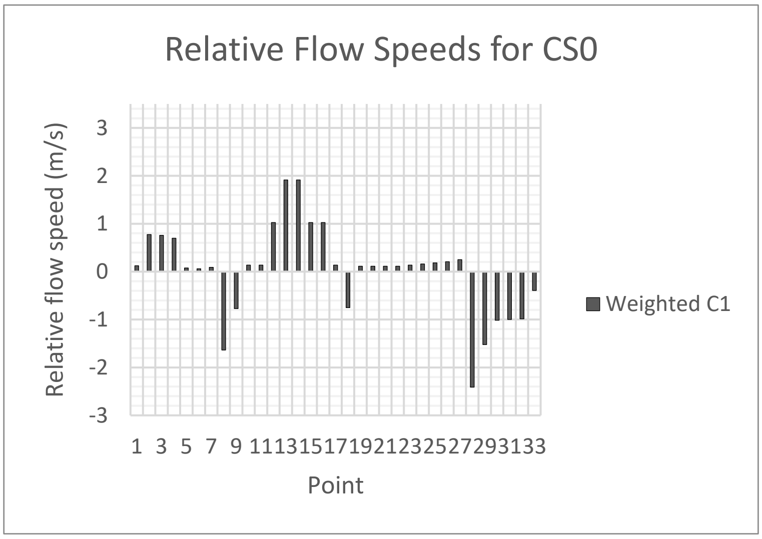

Figure 26: Weighted relative flow speeds for CS0 cross-section for the COMBINATION concept

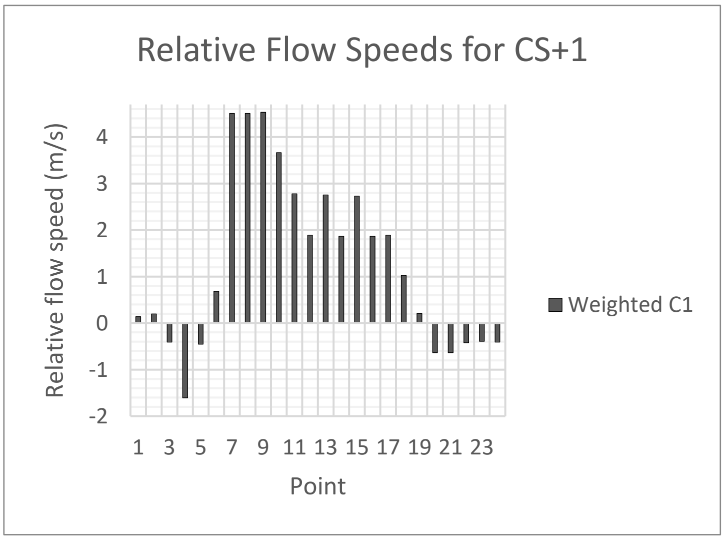

Figure 27: Weighted relative flow speeds for CS+1 cross-section for the COMBINATION concept

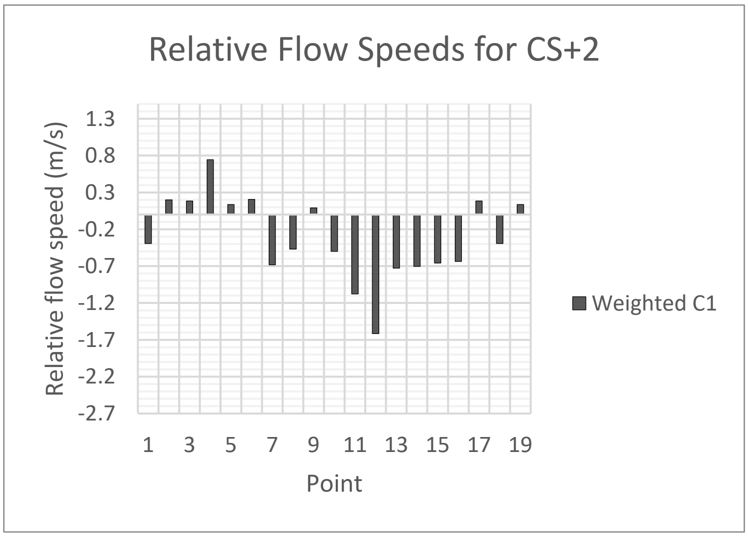

Figure 28: Weighted relative flow speeds for CS+2 cross-section for the COMBINATION concept

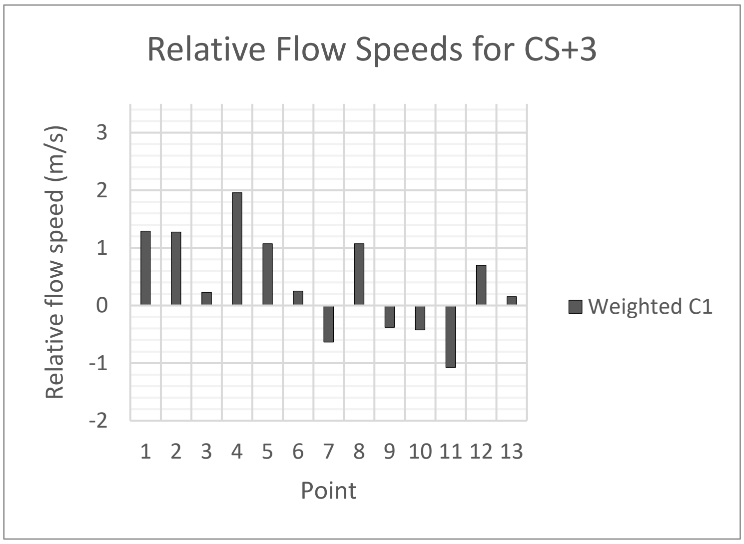

Figure 29: Weighted relative flow speeds for CS+3 cross-section for the COMBINATION concept

Table 3: Cross-section average flow speeds relative to baseline concept 0 (units: m/s)

Cross-section	F1	F2	F3	B1	B2	B3	S1	S2	S3	C1
CS0	-1.136	-0.345	0.070	0.359	-0.705	0.531	-0.624	-0.023	-0.072	0.018
CS+1	0.298	0.344	1.031	0.984	0.499	0.466	-0.104	0.434	-0.232	0.961
CS+2	-0.318	-0.417	-0.011	-0.076	-0.012	0.215	-0.338	0.036	0.084	-0.266
CS+3	0.337	0.151	-0.028	0.148	0.035	0.163	0.410	0.101	0.333	0.343
Relative average	-0.201	-0.049	0.242	0.342	-0.034	0.323	-0.149	0.159	0.071	0.225
% difference to C0 average	-4.18	-1.01	+5.02	+7.10	-0.70	+6.70	-3.09	+3.30	+1.47	+4.68

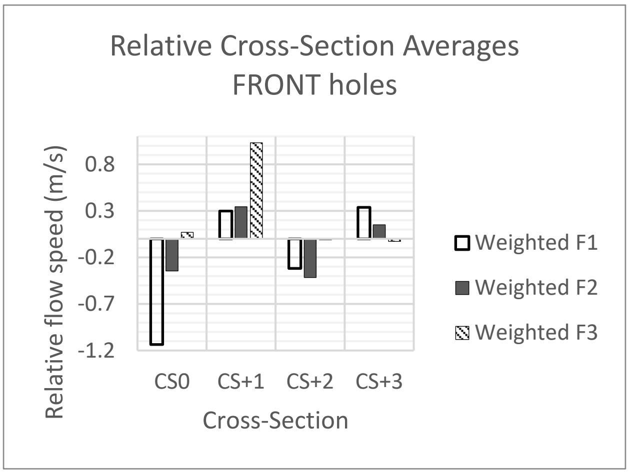

Figure 30: Relative Cross-section averages for the FRONT holes

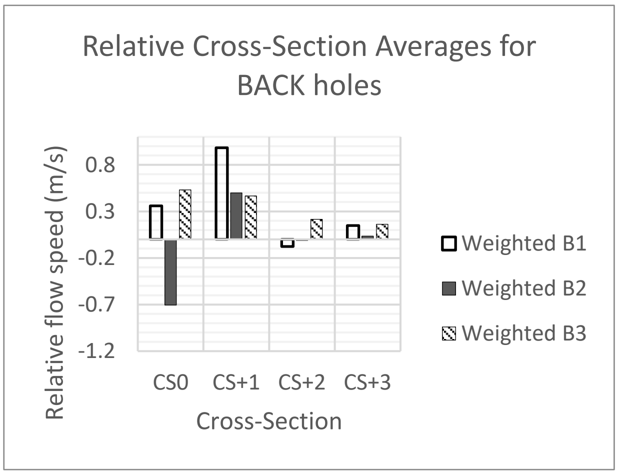

Figure 31: Relative Cross-section averages for the BACK holes

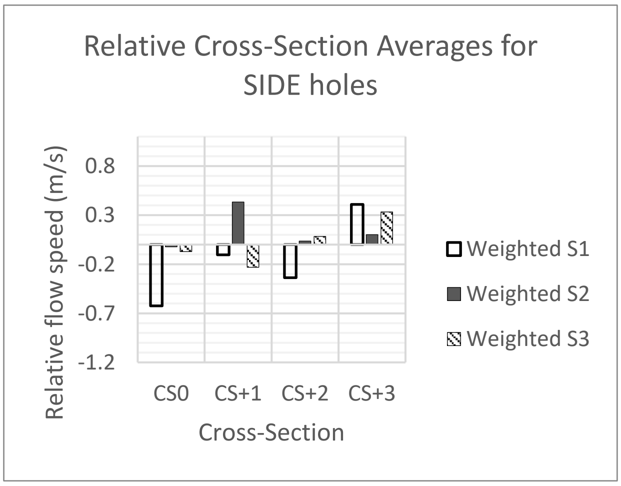

Figure 32: Relative Cross-section averages for the SIDE holes

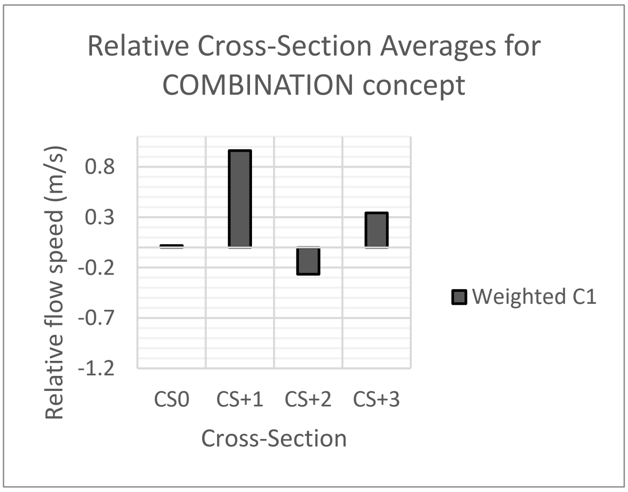

Figure 33: Relative Cross-section averages for the COMBINATION concept

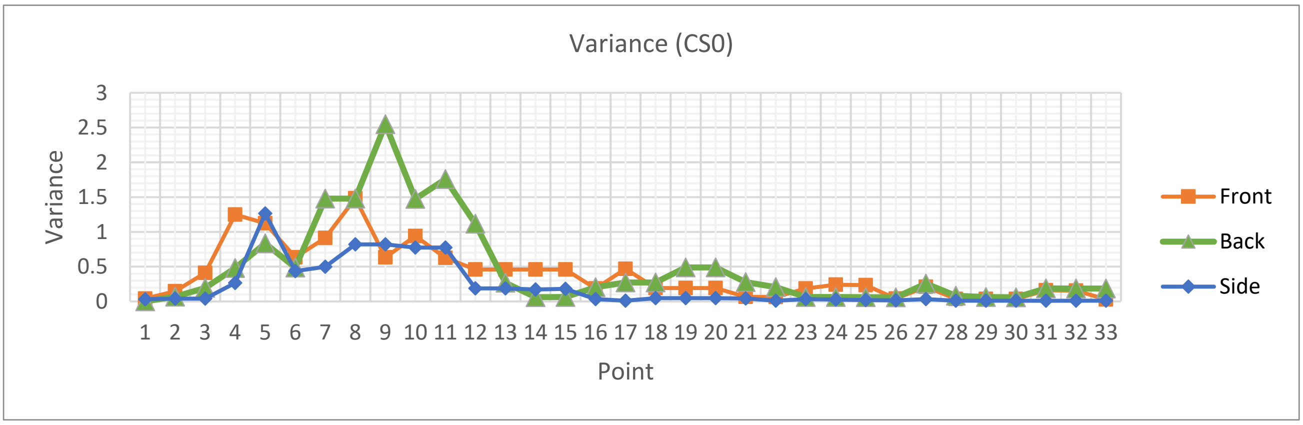

Figure 34: Variance of Airflow for CS0 Cross-Section

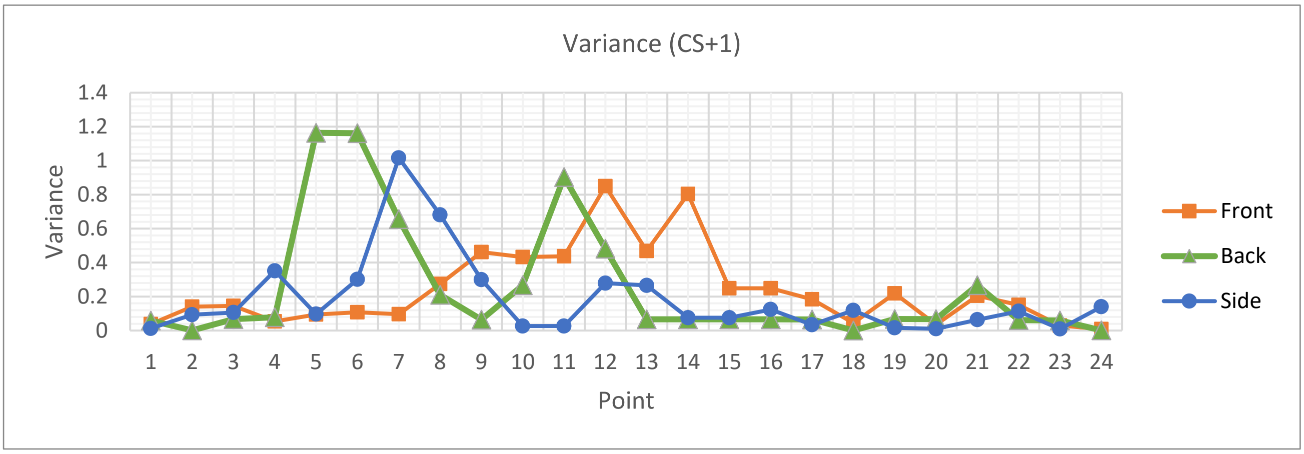

Figure 35: Variance of Airflow for CS+1 Cross-Section

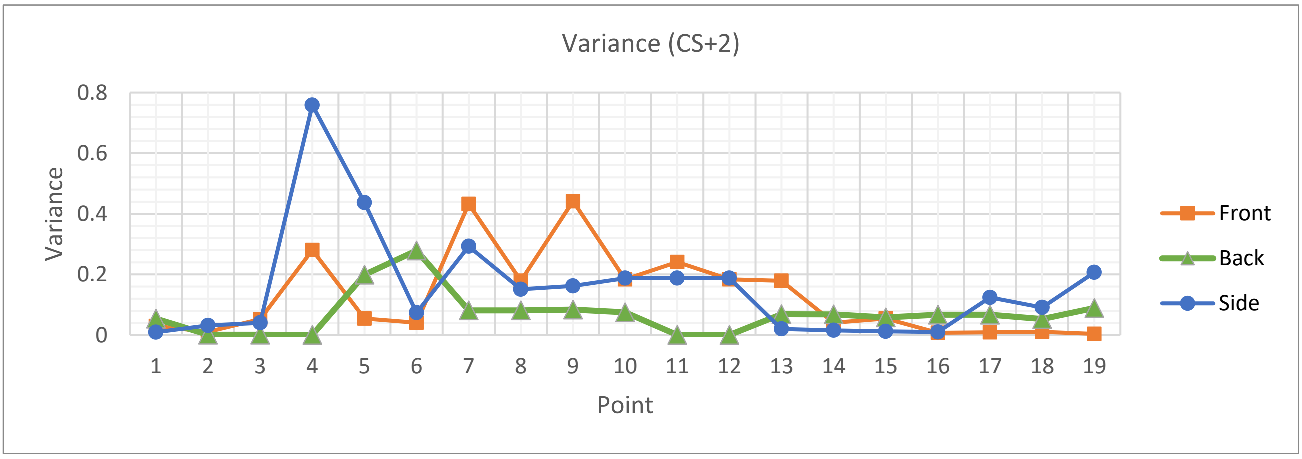

Figure 36: Variance of Airflow for CS+2 Cross-Section

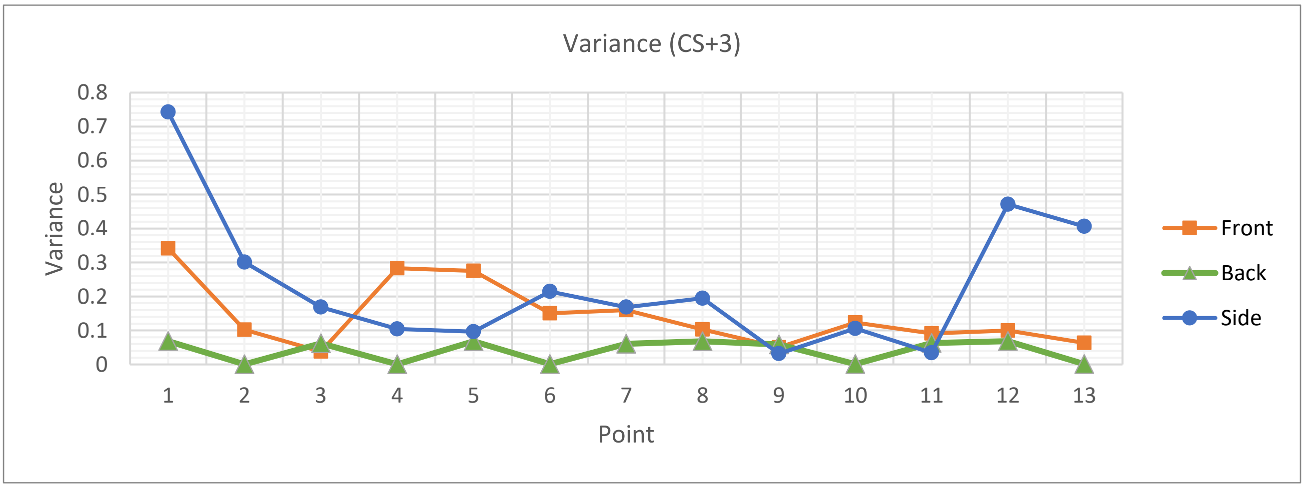

Figure 37: Variance of Airflow for CS+3 Cross-Section